Lattice dynamics of bcc Sr

J. Mizuki and C. Stassis

Ames Laboratory and Department of Physics, Iowa State University, Ames, Iowa 50011

(Received 26 June 1985)

A large single crystal of bcc Sr was grown *in situ* and was used to study the lattice dynamics of this divalent metal by coherent inelastic neutron scattering. The phonon dispersion curves were measured, at 930 K, along the $[\xi 00]$, $[\xi\xi 0]$, and $[\xi\xi\xi]$ symmetry directions. Along the $[\xi 00]$ symmetry direction, the frequencies of the longitudinal curve are higher than those of the transverse branch, whereas in bcc Ba, the relative ordering of these branches is reversed. This result is consistent with the assumption that the anomalous behavior of the $[\xi 00]$ dispersion curves in bcc Ba is due to the hybridization of the free-electron-like states with the d bands. The data were used to evaluate the elastic constants, the phonon density of states, and the lattice specific heat of bcc Sr.

I. INTRODUCTION

The electronic structure of the divalent alkaline-earth metals Ca, Sr, and Ba is quite simple.[1-5] Below the Fermi level E_F the electronic bands are practically free-electron-like. The d bands in these metals are only slightly above the Fermi level and, as a result, the electronic wave functions at E_F contain a substantial admixture of d character arising from hybridization of the free-electron-like states with the d bands. As a result, the structure and physical properties of these metals are quite sensitive[4,5] to the d occupation number.

Because of the relatively simple structure of these metals, it has been assumed that their lattice-dynamical properties can be adequately described within the framework of the pseudopotential theory of metals.[6,7] In recent experiments[8] on bcc Ba, however, it was found that along the $[\xi 00]$ symmetry direction the frequencies of the longitudinal dispersion curve are lower than those of the transverse branch. This anomalous feature of the dispersion curves was attributed[8] to the hybridization near the Fermi level of the free-electron-like states with the d bands. This interpretation has been supported[8] by first-principles frozen-phonon calculations. These calculations[8] showed, in addition, that the observed anomaly is quite sensitive to the position of the d bands relative to the Fermi level. Certainly, measurements of the dispersion curves of Sr, in which the d bands lie higher than in Ba, could provide additional support for this interpretation.

Strontium metal (which is fcc at room temperature) is stable in the bcc phase between approximately 830 K and its melting point (~ 1040 K). Recently, we were able to grow *in situ* single crystals of the bcc phase of Sr which were used to measure the phonon dispersion curves of this metal. In this Brief Report we present the results of these experiments.

II. EXPERIMENTAL DETAILS

Polycrystalline samples of high-purity Sr were encapsulated, under He, in thin-wall tantalum crucibles. To reduce the amount of hydrogen, which is the major impurity in Sr, the encapsulated samples were pumped for several weeks in a high vacuum at 950 °C (at this temperature hydrogen diffuses readily through tantalum).

The crystals were grown in a high-vacuum furnace positioned on the sample goniometer of a conventional triple-axis spectrometer at the Oak Ridge Reactor (ORR) of the Oak Ridge National Laboratory. Relatively large (several cubic centimeters) single crystals of the bcc phase were grown *in situ* by keeping the sample for several hours at a temperature just below the melting point, and then slowly cooling down to 930 K, the temperature at which we performed the measurements of the dispersion curves.

Most data were collected using the constant-Q method (Q is the neutron scattering vector), and constant scattered-neutron energies of 3.3 or 3.6 THz. A pyrolytic graphite filter was placed in the scattered beam to attenuate higher-order contaminations. Pyrolytic graphite [set to reflect from the (002) planes] was used as monochromator and analyzer, and 40' collimation was used before and after the sample. The measurements of the dispersion curves were performed in the $(1\bar{1}0)$ and $(1\bar{1}2)$ scattering planes.

III. EXPERIMENTAL RESULTS AND DISCUSSION

The phonon dispersion curves along the $[\xi 00]$, $[\xi\xi 0]$, and $[\xi\xi\xi]$ symmetry directions were measured at 930 K. The measured phonon frequencies are listed in Table I and the dispersion curves are plotted in Fig. 1.

It is instructive to compare the dispersion curves of bcc Sr with those[8] of bcc Ba. Along the $[\xi 00]$ symmetry direction the frequencies of the longitudinal curve are higher than those of the transverse branch in bcc Sr (Fig. 1), whereas in bcc Ba, the relative ordering of these branches is reversed. This result is consistent with the interpretation[8] that the anomalous behavior of the $[\xi 00]$ dispersion curves in Ba is due to the hybridization near the Fermi level of the d bands with the free-electron-like states. In Sr the d occupation number is considerably smaller than in Ba, and the normal ordering of the branches is restored, as predicted by first-principles frozen-phonon calculations.[8]

Another difference between the dispersion curves of Sr and Ba should be mentioned. The frequencies of the $T_1[\xi\xi 0]$ and $(2/3)[111]$ modes in Sr are lower than those obtained by scaling the frequencies of the corresponding Ba modes by the use of the Lindemann homology rule,[9] which takes into account the differences in mass, interatomic spac-

TABLE I. Measured phonon frequencies (THz) of bcc Sr at 930 K.

| ξ	ν
$L[00\xi]$	
0.1	0.41 ± 0.03
0.15	0.63 ± 0.02
0.2	0.85 ± 0.03
0.3	1.25 ± 0.02
0.4	1.57 ± 0.04
0.5	1.86 ± 0.05
0.6	2.20 ± 0.07
0.7	2.42 ± 0.07
0.8	2.44 ± 0.17
1.0	2.56 ± 0.12
$T[00\xi]$	
0.1	0.34 ± 0.02
0.15	0.53 ± 0.02
0.2	0.73 ± 0.02
0.3	1.06 ± 0.05
0.4	1.43 ± 0.07
0.5	1.77 ± 0.05
0.6	2.07 ± 0.05
0.7	2.30 ± 0.05
0.8	2.44 ± 0.09
0.9	2.54 ± 0.09
$T_1[\xi\xi0]$	
0.1	0.22 ± 0.01
0.15	0.33 ± 0.01
0.2	0.40 ± 0.02
0.3	0.56 ± 0.05
0.4	0.65 ± 0.05
0.5	0.71 ± 0.05
$T_2[\xi\xi0]$	
0.1	0.51 ± 0.01
0.15	0.77 ± 0.01
0.2	1.01 ± 0.04
0.3	1.45 ± 0.05
0.4	1.72 ± 0.05
0.5	1.83 ± 0.06
$L[\xi\xi0]$	
0.1	0.75 ± 0.05
0.15	1.11 ± 0.06
0.2	1.52 ± 0.05
0.3	2.16 ± 0.06
0.4	2.49 ± 0.10
0.5	2.61 ± 0.10
$T[\xi\xi\xi]$	
0.1	0.41 ± 0.02
0.15	0.65 ± 0.02
0.2	0.89 ± 0.02
0.3	1.33 ± 0.02
0.4	1.68 ± 0.05
0.5	1.99 ± 0.07
0.55	2.10 ± 0.05
0.6	2.24 ± 0.10
0.7	2.45 ± 0.07
0.8	2.50 ± 0.12
$L[\xi\xi\xi]$	
0.1	0.97 ± 0.02
0.15	1.50 ± 0.05
0.2	1.88 ± 0.07
0.3	2.35 ± 0.07
0.4	2.49 ± 0.05
0.5	1.99 ± 0.12
0.568	1.57 ± 0.04
0.633	1.21 ± 0.04
0.667	1.10 ± 0.05
0.715	1.21 ± 0.04
0.775	1.57 ± 0.04
0.825	1.93 ± 0.04
0.9	2.36 ± 0.06
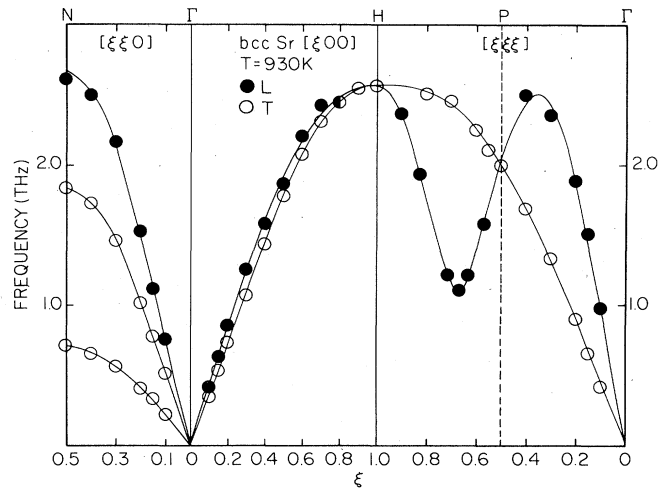
FIG. 1. Experimental dispersion curves of bcc Sr, at 930 K. The solid lines were obtained by fitting the data to a seven-nearest-neighbor force-constant model.

ing, and melting temperatures between Ba and Sr. This may be related to the fact that Sr, unlike Ba, undergoes a transformation at lower temperatures to the fcc structure. In fact, it appears that all bcc metals which undergo a martensitic transformation to a close-packed structure at some lower temperature are characterized by low frequencies for the $T_1[\xi\xi0]$ and $(2/3)[111]$ vibrational modes.

No first-principles calculations of the dispersion curves of bcc Sr are available for a detailed comparison with the experimental results. Pseudopotential calculations were performed by Animalu,[6] using a local pseudopotential. Except for the $T_1[\xi\xi0]$ branch, the calculated[6] frequencies are substantially higher than the measured values.

To evaluate the elastic constants and lattice specific heat,

TABLE II. Atomic force constants and elastic constants obtained by fitting the data to a seven-nearest-neighbor model.

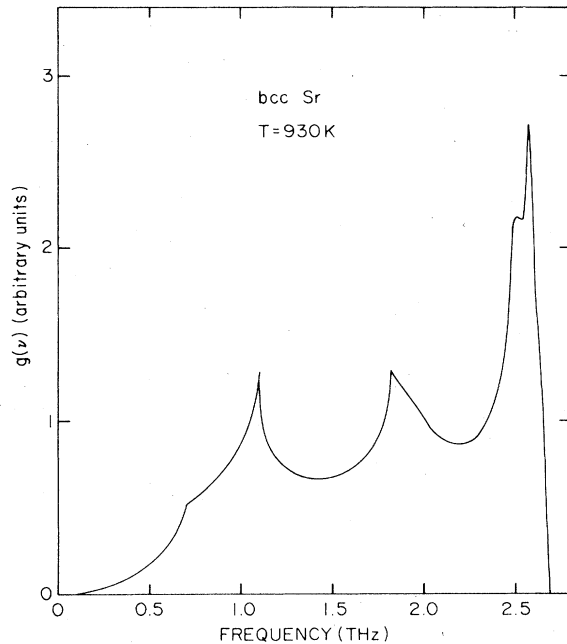| Atomic force constants (dyn/cm)			Elastic constants (10^{12} dyn/cm^2)	
$1XX$	2387.3 ±	41.0	C_{11}	0.081 18
$1XY$	2623.1 ±	74.8		
$2XX$	588.5 ±	145.7		
$2YY$	799.3 ±	69.5	C_{44}	0.101 08
$3XX$	−332.5 ±	37.6		
$3ZZ$	384.6 ±	76.4	$(1/2)(C_{11}-C_{12})$	0.042 47
$3XY$	0.1 ±	70.6		
$4XX$	176.0 ±	63.4		
$4YY$	22.3 ±	37.1		
$4YZ$	−47.0 ±	43.2		
$4XZ$	26.1 ±	37.6		
$5XX$	−186.2 ±	35.8		
$5XY$	−112.5 ±	61.4		
$6XX$	133.1 ±	131.1		
$6YY$	13.3 ±	66.9		
$7XX$	−57.4 ±	24.5		
$7ZZ$	13.2 ±	35.5		
$7YZ$	−55.2 ±	31.3		
$7XY$	−55.0 ±	31.0		

FIG. 2. Phonon density of states $g(\nu)$ of bcc Sr at 930 K, evaluated using the force constants listed in Table II.

FIG. 3. Temperature dependence of the effective Debye temperature of bcc Sr, evaluated using the phonon density of states plotted in Fig. 2.

we analyzed the data by conventional Born–von Kármán force-constant models. It can be seen (Fig. 1) that a seven-nearest-neighbor force-constant model provides an adequate fit to the experimental data. The force and elastic constants obtained by fitting the data to this model are listed in Table II. Using the force constants listed in Table II, the phonon density of states was evaluated (Fig. 2) by the method of Gilat and Raubenheimer.[10] The lattice specific heat, expressed in terms of an effective Debye temperature
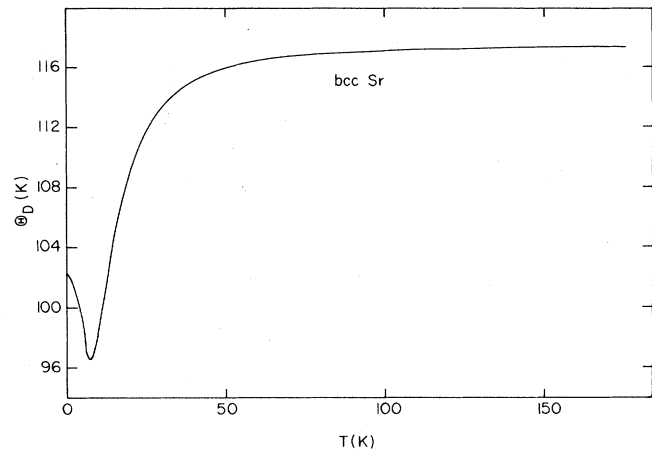
$\Theta_D(T)$, was evaluated (Fig. 3) by assuming that the phonon density of states was independent of temperature. No experimental data are presently available for a detailed comparison with the results of the present analysis.

[1]B. Vasvari, A. O. E. Animalu, and V. Heine, Phys. Rev. B 154, 535 (1967).
[2]G. Johansen, Solid State Commun. 7, 731 (1969).
[3]J.-P. Jan and H. L. Skriver, J. Phys. F 11, 805 (1981).
[4]H. L. Skriver, Phys. Rev. Lett. 49, 1768 (1982).
[5]H. L. Skriver, Phys. Rev. B 31, 1909 (1985).
[6]A. O. E. Animalu, Phys. Rev. 161, 445 (1967).

[7]J. A. Moriarty, Phys. Rev. B 6, 4445 (1972); 8, 1338 (1973); 16 2537 (1977); 26, 1754 (1982); 28, 4818 (1983).
[8]J. Mizuki, Y. Chen, K.-M. Ho, and C. Stassis, Phys. Rev. B 32, 666 (1985).
[9]F. A. Lindemann, Phys. Z. 11, 609 (1910).
[10]G. Gilat and L. T. Raubenheimer, Phys. Rev. 144, 390 (1966).